

Identification of functional pathways associated with the conditional ablation of serum response factor in *Dstn^{corn1}* mice

YANAN HUO¹, XIN XIE¹ and BO JIANG²

¹Eye Center, Second Affiliated Hospital of Zhejiang University School of Medicine, Hangzhou, Zhejiang 310009;

²Department of Ophthalmology, First Affiliated Hospital, College of Medicine, Zhejiang University, Hangzhou, Zhejiang 310003, P.R. China

Received October 9, 2015; Accepted July 25, 2016

DOI: 10.3892/mmr.2016.5984

Abstract. The aim of the present study was to investigate the signaling pathways associated with functional alterations in corneal tissues following the conditional ablation of serum response factor (*Srf*) in *Dstn^{corn1}* mice. The gene expression profiling array GSE49688, which includes 3 samples each from the wild-type (WT), *Dstn^{corn1}* mutant (*corn1*) and *corn1* mice following the conditional ablation of *Srf* from the corneal epithelium [namely rescued (*res*)] mouse groups, was downloaded from the Gene Expression Omnibus database. The limma package was used to identify differentially expressed genes (DEGs) among the three mouse groups. DEGs were subsequently analyzed by dynamic comparison, hierarchical clustering and pathway enrichment analysis. Pathway alteration scores were also calculated in order to study the dynamic metergasis of each identified pathway. A total of 788 DEGs were identified between the *corn1* and *res* groups, 1,365 DEGs were identified between the *corn1* and WT groups, and 852 DEGs were identified between the *res* and WT groups. Among these DEGs, 228 genes were differentially expressed across all three groups, and were mainly enriched in signaling pathways involved in the regulation of the actin cytoskeleton, including the cofilin 1 (*CFL1*), the mitogen-activated protein kinase (MAPK) signaling pathway and focal adhesion. The dilated cardiomyopathy signaling pathway displayed the highest alteration score, and was enriched with integrin and integrin β -6 (*ITGB6*). In conclusion, the actin cytoskeleton regulatory pathway, MAPK and dilated cardiomyopathy signaling pathways, as well as *CFL1* and *ITGB6* genes, may be regulated by *Srf* to serve important roles in the progression of corneal disease.

Introduction

Epithelial hyperproliferation, increased angiogenesis and inflammation are biological processes associated with the pathogenesis of corneal disease, and are the primary cause of bilateral blindness worldwide (1,2). In addition, a number of other disease conditions may arise as a result of abnormal epithelial cell proliferation, inflammation and angiogenesis, such as tumorigenesis and chronic inflammatory disorders (3,4). As a result, investigating the molecular mechanisms underlying these conditions is of critical importance.

Dstn^{corn1} mice are homozygous for a spontaneous null actin depolymerizing factor destrin (DSTN) allele, which results in an increase in serum response factor (*Srf*) expression. This increase in *Srf* production may lead to corneal abnormalities, including epithelial hyperproliferation, neovascularization and inflammation in the cornea (5). Based on these characteristics, *Dstn^{corn1}* mice often serve as suitable *in vivo* models for the investigation of corneal diseases (6). Verdoni *et al* (1) demonstrated that conditional *Srf* knockout in the corneal epithelium of *Dstn^{corn1}* mice rescues epithelial cell hyperproliferation, neovascularization and inflammatory phenotypes. In addition, previous studies have demonstrated that vascular endothelial growth factor receptor 1 (VEGFR1) was downregulated in *Dstn^{corn1}* mice (7) and that conditional *Srf* knockout *Dstn^{corn1}* mice displayed increased levels of VEGFR1 (1). The genome-wide screening of differentially expressed genes (DEGs) in the corneas of *Dstn^{corn1}* mice has revealed that a large proportion of upregulated DEGs are targets of *Srf* (8). Additionally, another study by Verdoni *et al* (9) indicated that the B-cell receptor signaling pathway served an important role in the phenotype of *Dstn^{corn1}* mice. Although a considerable number of studies have focused on understanding the molecular mechanisms of the *Dstn^{corn1}* phenotype, the development of various abnormalities remains unclear.

Kawakami-Schulz *et al* (5) identified the gene networks that were affected by the increased expression of *Srf* in *Dstn^{corn1}* mouse corneas. The expression profiling array GSE49688, which was provided by Kawakami-Schulz *et al* (5), was downloaded for analysis in the present study. The aim of the present study was to identify DEGs and perform signaling pathway analysis among three types of mice included in the GSE49688 array using various bioinformatics tools. The

Correspondence to: Dr Yanan Huo, Eye Center, Second Affiliated Hospital of Zhejiang University School of Medicine, 88 Jiefang Road, Hangzhou, Zhejiang 310009, P.R. China
E-mail: yananhuo@sina.com

Key words: corneal disease, serum response factor, differentially expressed genes, pathway enrichment analysis, pathway alteration score

results may provide an important theoretical foundation for understanding the role of *Srf* in normal and abnormal corneal tissue homeostasis.

Materials and methods

Affymetrix microarray data. Data from the expression profiling array GSE49688 (5) were downloaded from the Gene Expression Omnibus database (<http://www.ncbi.nlm.nih.gov/geo/>). This dataset is based on the GPL16570 MoGene-2_0-st Affymetrix Mouse Gene 2.0 ST Array [transcript (gene) version] platform (Affymetrix, Inc., Santa Clara, CA, USA). In total, 9 samples are included in the datasets, with 3 samples each from the following groups: i) Wild-type (WT) mice; ii) a *Dstn*^{corn1} mutant mouse model of corneal disease; and iii) *Dstn*^{corn1} mutant mice following the conditional ablation of *Srf* from the corneal epithelium [namely the rescued (res) group].

Data preprocessing and differential expression analysis. The expression profiling probes were first annotated through annotation files. Subsequently, gene symbols were identified from annotation files, with the use of editing codes. Next, expression profiling of gene symbols was performed by Z-score normalization, as previously described (10). The linear models for microarray data (limma) version 3.28.17 (11) in R-software package (www.r-project.org) were applied to identify the DEGs among the three mouse groups. The log₂-fold change (log₂FC) and the false discovery rate (FDR) (12) were calculated. Genes with log₂FC>1 and an FDR <0.05 were considered to be DEGs and were used for subsequent analysis.

Dynamic comparison and hierarchical cluster analyses of DEGs. In order to verify that the three mouse groups represented three distinct states and examine their correlation at a molecular level, dynamic comparisons and unsupervised clustering analyses of DEGs were performed for the 9 samples in the GSE49688 array. DEGs between two mouse groups were determined at a time, thus obtaining three DEG groups, namely the corn1 vs. WT, res vs. corn1 and res vs. WT groups. The common DEGs among the three groups were then clustered hierarchically (13) and visualized using the TreeView program (jtreeview.sourceforge.net/) (14), and genes and samples were normalized using the median center method (15). The similarity matrix used the correlation-centered metric (16).

Pathway enrichment analysis. The Kyoto Encyclopedia of Genes and Genomes (KEGG; www.genome.ad.jp/kegg/) (17) knowledge database is a collection of online databases of genomes, enzymatic pathways and biological chemicals. In the present study, KEGG pathway enrichment analysis for the three groups of DEGs was performed. In addition, their association based on function was determined using the Database for Annotation, Visualization and Integrated Discovery (DAVID; <http://david.abcc.ncifcrf.gov>) gene classification tool (18). P<0.05 was established as the threshold for the hypergeometric test.

Pathway alteration score. Quantitative scoring was performed for the potential pathways based on genes enriched in the

pathway. The Euclidean distance quantitative method was used to calculate the dynamic metergasis of pathways in the corn1 and res phenotypes compared with the WT phenotype (19). The pathway alteration score was calculated using the following formula:

$$A(P) = \log_{10} \left(\frac{1}{N} \sum_{i=1}^N \sqrt{(X_{gene} - Y_{gene})^2} \right),$$

where A(P) is the alteration score of the pathway, N is the number of DEGs, X_{gene} is the expression value of gene in the corn1 or res phenotypes and Y_{gene} is the expression value of gene in the WT phenotype group. The higher the score, the clearer the alteration degree of pathway from WT phenotype.

Results

Identification of DEGs. A pairwise comparison of genes from the WT, corn1 and res sample groups was performed in order to identify the DEGs between groups. As presented in Fig. 1A, a total of 1,365 DEGs were identified between the corn1 and WT sample groups, including 867 upregulated and 498 downregulated DEGs. Between the corn1 and res sample groups, 788 DEGs were identified, including 345 upregulated and 443 downregulated DEGs (Fig. 1B). A total of 852 DEGs were identified between the res and WT sample groups, including 593 upregulated and 259 downregulated DEGs (Fig. 1C).

Dynamic comparison and hierarchical cluster analysis of DEGs. Dynamic comparison analysis of DEGs among sample groups revealed that the number of DEGs between corn1 and WT was the greatest (n=1,365). Among these, 826 genes overlapped with DEGs identified in the res vs. WT group, 763 genes overlapped with DEGs identified in the res vs. corn1 group, whereas only 6 genes were specific to the corn1 vs. WT group (Fig. 2). In addition, 228 common genes were differentially expressed across all three groups (Fig. 2). These results reflected the differences in expression between the three sample groups, with the res phenotype representing the transition state between WT and corn1 groups.

Hierarchical cluster analysis results are shown in Fig. 3. The cluster analysis demonstrated that the three groups exhibited distinct gene expression patterns, and confirmed that the res phenotype represented a transition state between WT and corn1 groups.

KEGG pathway enrichment analysis. The KEGG signaling pathways enriched by the upregulated and downregulated DEGs are shown in Table I. In the corn1 vs. WT and the res vs. WT groups, the upregulated DEGs were mainly enriched in the cytokine-cytokine receptor interaction and cell adhesion molecule signaling pathways, while the downregulated DEGs were mainly enriched in signaling pathways associated with cellular metabolism. Upregulated DEGs in the res vs. corn1 group were enriched in the retinol metabolism pathway, while downregulated DEGs were primarily enriched in the regulation of actin cytoskeleton (cofilin1 (*CFL1*) and *CFL2*) and mitogen-activated protein kinase (MAPK) signaling

Table I. KEGG pathway enrichment analysis showing the identified DEGs among the various mouse groups.

KEGG term	Count ^a	P-value
A, Upregulated DEGs		
Corn1 vs. WT		
mmu04060: Cytokine-cytokine receptor interaction	47	9.47x10 ⁻¹⁷
mmu04514: CAMs	21	3.32x10 ⁻⁵
mmu04670: Leukocyte transendothelial migration	18	3.84x10 ⁻⁵
mmu04062: Chemokine signaling pathway	23	4.15x10 ⁻⁵
mmu05322: Systemic lupus erythematosus	16	8.80x10 ⁻⁵
Res vs. WT		
mmu04060: Cytokine-cytokine receptor interaction	41	1.17x10 ⁻¹⁷
mmu04640: Hematopoietic cell lineage	14	4.05x10 ⁻⁶
mmu04670: Leukocyte transendothelial migration	16	1.00x10 ⁻⁵
mmu04062: Chemokine signaling pathway	19	3.89x10 ⁻⁵
mmu04514: CAMs	17	5.86x10 ⁻⁵
Res vs. corn1		
mmu00830: Retinol metabolism	4	4.62x10 ⁻²
B, Downregulated DEGs		
Corn1 vs. WT		
mmu00830: Retinol metabolism	8	1.71x10 ⁻⁴
mmu00982: Drug metabolism	7	1.93x10 ⁻³
mmu00980: Metabolism of xenobiotics by cytochrome P450	6	5.85x10 ⁻³
mmu04710: Circadian rhythm	3	2.11x10 ⁻²
mmu00071: Fatty acid metabolism	4	4.41x10 ⁻²
Res vs. WT		
mmu00830: Retinol metabolism	5	5.03x10 ⁻³
mmu00982: Drug metabolism	5	7.12x10 ⁻³
mmu04710: Circadian rhythm	3	7.54x10 ⁻³
mmu00980: Metabolism of xenobiotics by cytochrome P450	4	2.99x10 ⁻²
Res vs. corn1		
mmu04810: Regulation of actin cytoskeleton	16	1.43x10 ⁻⁴
mmu04510: Focal adhesion	13	2.14x10 ⁻³
mmu04010: MAPK signaling pathway	14	8.59x10 ⁻³
mmu04270: Vascular smooth muscle contraction	8	2.17x10 ⁻²
mmu00052: Galactose metabolism	4	2.42x10 ⁻²
C, Overlapping DEGs (n=228)		
mmu04510: Focal adhesion	8	1.64x10 ⁻²
mmu04010: MAPK signaling pathway	8	2.38x10 ⁻²
mmu04810: Regulation of actin cytoskeleton	7	3.01x10 ⁻²
^a Count is the number of DEGs associated with each term. KEGG, Kyoto Encyclopedia of Genes and Genomes; DEG, differentially expressed gene; WT, wild-type; corn1, Dstn ^{corn1} mutant mice; res, serum response factor knockout in Dstn ^{corn1} mutant mice; Dstn, destrin; CAMs, cell adhesion molecules; MAPK, mitogen-activated protein kinase.		

pathways. In addition, the 228 overlapping DEGs among the three groups were mainly enriched in the focal adhesion, MAPK and regulation of actin cytoskeleton signaling pathways.

Pathway alteration score. The pathway alteration scores of the WT, corn1 and res groups are shown in Fig. 4, and the 10 most altered pathways among the three groups are shown in Table II. Distance scores in Table II indicate the degree of deviation

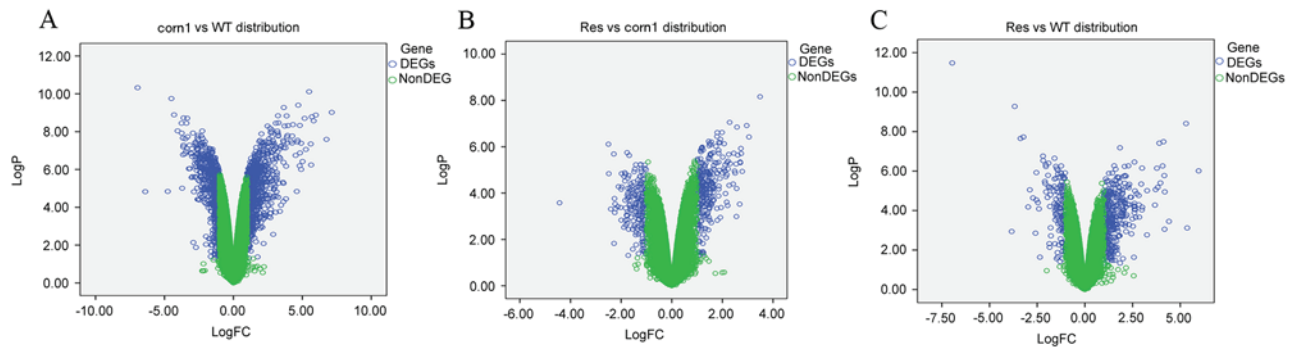


Figure 1. Volcano plots of microarray gene expression data obtained following the comparison of (A) *corn1* vs. WT, (B) *res* vs. *corn1* and (C) *res* vs. WT groups. The y-axis indicates the $-\log_{10}$ of P-values. DEG, differentially expressed gene; WT, wild-type; *Dstn*, destrin; FC, fold change; *corn1*, *Dstn^{corn1}* mutant mice; *res*, serum response factor knockout in *Dstn^{corn1}* mutant mice.

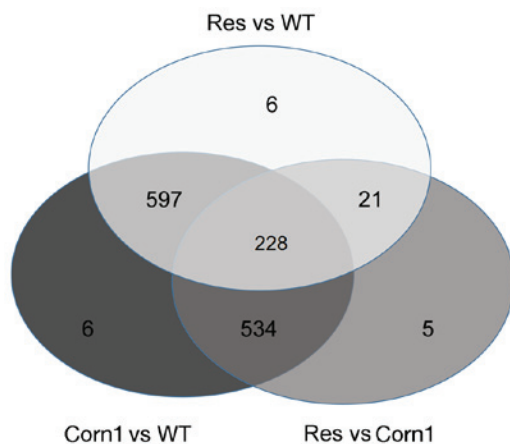


Figure 2. Venn diagram showing the differentially expressed genes among the *res* vs. WT, *res* vs. *corn1* and *corn1* vs. WT groups. WT, wild-type; *Dstn*, destrin; *corn1*, *Dstn^{corn1}* mutant mice; *res*, serum response factor knockout in *Dstn^{corn1}* mutant mice.

between *corn1* or *res* groups from the WT group that is the absolute difference value between the *corn* and *res* scores. WT group served as a reference, and a high score indicated a greater degree of alteration, whereas a low score indicated that *corn1* or *res* group mice were closer to the WT state. The pathways associated with the cardiovascular system, glycometabolism and the inflammatory response exhibited high pathway alteration scores. Of these, the dilated cardiomyopathy signaling pathway demonstrated the greatest score, and was enriched by particular DEGs, including integrin beta 6 (*ITGB6*).

Discussion

Srf activation has been reported to be involved in angiogenesis, the maintenance of cell hyperproliferation, inflammation and F-actin accumulation in *Dstn^{corn1}* mice (20). Notably, *Srf* is known to be involved in the pathogenesis of multiple types of cancer, including hepatocellular and colorectal cancer, demonstrating its potential as a disease-causing factor (21,22). In the present study, 228 common genes were differentially expressed in the three groups (WT, *corn1* and *res*), and were mainly enriched in the focal adhesion, MAPK and regulation of actin cytoskeleton signaling pathways. In addition, pathways

Table II. Pathway alteration scores for the deviation of *corn1* and *res* groups from the WT group.

Pathway	Corn1	Res	Distance ^a
Dilated cardiomyopathy	-0.1	-0.53	0.43
Vascular smooth muscle contraction	-0.32	-0.73	0.41
Fructose and mannose metabolism	0.05	-0.31	0.36
Galactose metabolism	0.05	-0.31	0.36
MAPK signaling pathway	-0.24	-0.59	0.35
Regulation of actin cytoskeleton	-0.36	-0.67	0.31
Arachidonic acid metabolism	0	-0.26	0.26
Systemic lupus erythematosus	-0.57	-0.82	0.25
Fatty acid metabolism	0.05	-0.2	0.25
Focal adhesion	-0.34	-0.58	0.24

^aDistance is the absolute difference value between the *corn* and *res* scores, with a higher value indicating a more altered pathway compared with WT. DEG, differentially expressed gene; WT, wild-type; *corn1*, *Dstn^{corn1}* mutant mice; *res*, serum response factor knockout in *Dstn^{corn1}* mutant mice; *Dstn*, destrin; MAPK, mitogen-activated protein kinase.

associated with the cardiovascular system, glycometabolism and the inflammatory response displayed high pathway alteration scores. These results may improve our understanding of the role of *Srf* in normal and abnormal corneal tissue homeostasis.

In the present study, the actin cytoskeleton pathway was demonstrated to be a significant pathway. In addition, overlapping DEGs in all three groups were enriched for this pathway. The actin cytoskeleton is essential for the maintenance of cell morphology and mechanical support, as well as for the regulation of diverse processes, including apoptosis, cell adhesion, cell migration and phagocytosis (23). Furthermore, the actin cytoskeleton is a critical barrier between the external environment of surrounding cells and the internal cell signaling pathways, which ultimately affects gene expression regulation (5). Ikeda *et al.* (24) suggested that the appropriate regulation of actin dynamics is necessary for the normal maintenance of the corneal epithelium, and aberrant regulation of the actin cytoskeleton leads to epithelial cell proliferation.

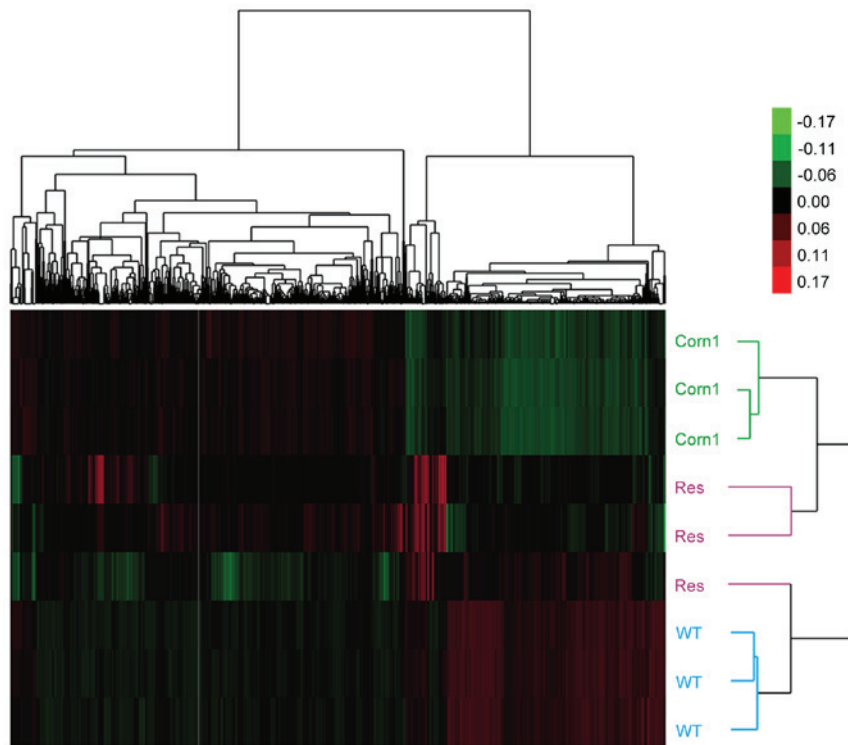


Figure 3. Hierarchical cluster analysis heat map of overlapping differentially expressed genes among the WT, *corn1* and *res* groups. Red signals indicate increased expression and green signals indicate reduced expression. WT, wild-type; *Dstn*, destrin; *corn1*, *Dstn^{corn1}* mutant mice; *res*, serum response factor knockout in *Dstn^{corn1}* mutant mice.

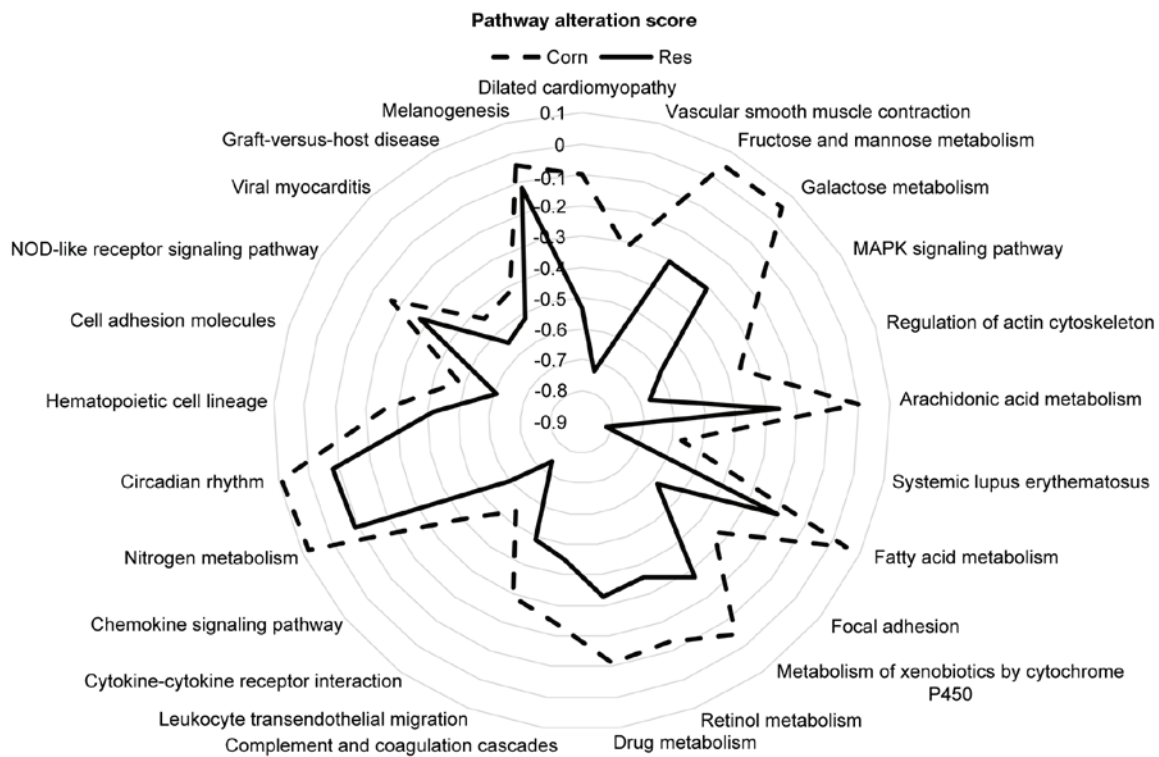


Figure 4. Pathway alteration scores in *corn1* mice vs. WT, and *res* vs. WT groups. The dashed-line indicates the degree of deviation between *corn1* and WT mice, and the filled-line indicates the degree of deviation between *res* mice and WT mice. *Dstn*, destrin; WT, wild-type; MAPK, mitogen-activated protein kinase; *corn1*, *Dstn^{corn1}* mutant mice; *res*, serum response factor knockout in *Dstn^{corn1}* mutant mice.

Notably, *Srf* is an essential regulator of the actin cytoskeleton, and *Srf* target genes are known to be regulated by dynamic

changes in the actin cytoskeleton (8,25). Thus, mutant *Srf*-mediated regulation of the actin cytoskeleton pathway may

serve an important role in the development of corneal disease in *Dstn^{corn1}* mutant mice.

Previous studies have demonstrated that proteins encoded by particular *Srf* target genes, such as *CFL1* and *CFL2*, serve key roles in actin treadmilling (26,27). In the present study, *CFL1* was enriched in the actin cytoskeleton regulatory pathway. *CFL1* is a member of the actin depolymerizing factor/CFL family and is a primary regulator of actin dynamics (28). It is ubiquitously expressed and is crucial for efficient actin depolymerization (29). Notably, Ikeda *et al* (24) demonstrated that *CFL1* and *DSTN* have common functions; however, compensatory mechanisms following functional loss of one actin depolymerizing factor are insufficient to restore normal actin dynamics in the cornea. Therefore, despite observing an upregulation of *CFL1* in the *res* group compared with the *corn1* group in the present study, *CFL1* may have been unable to completely regulate actin filament dynamics and compensate for the loss of *DSTN*.

Cell hyperproliferation, angiogenesis and inflammation are biological processes involved in the pathogenesis of corneal disease, as well as in chronic inflammatory disorders and tumorigenesis (3,4). Therefore, it is possible that signaling pathways associated with cancer may be involved in the progression of corneal disease in *Dstn^{corn1}* mutant mice. For instance, the MAPK signaling pathway was significant in the current study. Signaling to *Srf* occurs principally through the MAPK signaling pathway, which stimulates the expression of cell growth-promoting genes that encode proteins responsible for directly activating genes involved in cell cycle progression and growth factors (30,31). Cell cycle regulation is known to be critical for the normal proliferation and development of multicellular organisms (32). The MAPK pathway is frequently activated in human cancer, which can lead to a malignant phenotype through increased cell proliferation (33). In the present study, the MAPK signaling pathway was enriched by particular downregulated DEGs in the *res* sample group, which indicates that *Srf* knockout may have affected the function of this pathway. In addition, pathway alteration analysis demonstrated that the dilated cardiomyopathy signaling pathway exhibited the highest score, and *ITGB6* was revealed to be enriched in this pathway.

Integrins, consisting of α and β subunits, are a family of cell surface receptors that mediate cell-to-cell adhesion (34,35). Notably, integrins have been reported to contribute to cell proliferation, apoptosis and the regulation of gene expression, and have been suggested to serve important roles in inflammation and tumorigenesis (34,36). In the present study, *ITGB6* was observed to be downregulated in the *res* group compared with the *corn1* group, which indicated that *ITGB6* may be targeted by *Srf*. *ITGB6* is expressed specifically in epithelial cells (34); thus, epithelial hyperproliferation in the *Dstn^{corn1}* mice may be induced by upregulation of *ITGB6*. Ultimately, the dilated cardiomyopathy signaling pathway and *ITGB6* may serve important roles in the process of epithelial hyperproliferation and inflammation in the corneas of *Dstn^{corn1}* mice.

In conclusion, the results of the present study provide a comprehensive bioinformatics analysis of DEGs and signaling pathways involved in the dynamic process of *Dstn^{corn1}* mice returning to a WT-like state following the conditional ablation of *Srf* from the corneal epithelium. The actin cytoskeleton, MAPK and dilated cardiomyopathy signaling pathways, as

well as *CFL1* and *ITGB6* DEGs, may be regulated by *Srf* to serve important roles in corneal disease progression. These results may increase our understanding on the role of *Srf* in corneal disease tissues. However, further genetic and experimental studies with larger sample sizes are required to confirm the results of the present study, and to identify therapeutic targets for the treatment of corneal diseases.

Acknowledgements

The present study was supported by the National Natural Science Foundation of China (grant no. 81200662), the Zhejiang Provincial Natural Science Foundation of China (grant nos. LY12H12010 and LY13H120002) and the Project of Zhejiang Provincial Department of Health (grant no. 2013KYB141).

References

- Verdoni AM, Schuster KJ, Cole BS, Ikeda A, Kao WW and Ikeda S: A pathogenic relationship between a regulator of the actin cytoskeleton and serum response factor. *Genetics* 186: 147-157, 2010.
- Li Z, Cui H, Zhang L, Liu P and Bai J: Prevalence of and associated factors for corneal blindness in a rural adult population (the southern Harbin eye study). *Curr Eye Res* 34: 646-651, 2009.
- Allavena P, Garlanda C, Borrello MG, Sica A and Mantovani A: Pathways connecting inflammation and cancer. *Curr Opin Genet Dev* 18: 3-10, 2008.
- D'Aura Swanson C, Paniagua RT, Lindstrom TM and Robinson WH: Tyrosine kinases as targets for the treatment of rheumatoid arthritis. *Nat Rev Rheumatol* 5: 317-324, 2009.
- Kawakami-Schulz SV, Verdoni AM, Sattler SG, Jessen E, Kao WW, Ikeda A and Ikeda S: Serum response factor: Positive and negative regulation of an epithelial gene expression network in the destrin mutant cornea. *Physiol Genomics* 46: 277-289, 2014.
- Zhou Q, Li Y and Chen B: The effect of destrin mutations pathways on the gene expression profile. *African Journal of Pharmacy and Pharmacology* 6: 1746-1752, 2012.
- Qazi Y, Wong G, Monson B, Stringham J and Ambati BK: Corneal transparency: Genesis, maintenance and dysfunction. *Brain Res Bull* 81: 198-210, 2010.
- Miano JM: SRF'ing the actin cytoskeleton with no destrin. *Physiol Genomics* 34: 6-8, 2008.
- Verdoni AM, Aoyama N, Ikeda A and Ikeda S: Effect of destrin mutations on the gene expression profile in vivo. *Physiol Genomics* 34: 9-21, 2008.
- Murie C, Barette C, Lafanechère L and Nadon R: Control-Plate Regression (CPR) normalization for high-throughput screens with many active features. *J Biomol Screen* 19: 661-671, 2014.
- Diboun I, Wernisch L, Orengo CA and Koltzenburg M: Microarray analysis after RNA amplification can detect pronounced differences in gene expression using limma. *BMC Genomics* 7: 252, 2006.
- Jahani M, Nematzadeh G, Dolatabadi B, Hashemi SH and Mohammadi-Nejad G: Identification and validation of functional markers in a global rice collection by association mapping. *Genome* 57: 355-362, 2014.
- Petushkova NA, Pyatnitskiy MA, Rudenko VA, Larina OV, Trifonova OP, Kisrieva JS, Samenkova NF, Kuznetsova GP, Karuzina II and Lisitsa AV: Applying of hierarchical clustering to analysis of protein patterns in the human cancer-associated liver. *PLOS One* 9: e103950, 2014.
- Zhai Y, Tchieu J and Saier MH Jr: A web-based tree view (TV) program for the visualization of phylogenetic trees. *J Mol Microbiol Biotechnol* 4: 69-70, 2002.
- Di Pietro C, Di Pietro V, Emmanuele G, Ferro A, Maugeri T, Modica E, Pigola G, Pulvirenti A, Purrello M, Ragusa M, *et al*: Anticlustal: Multiple sequence alignment by antipole clustering and linear approximate 1-median computation. *Proc IEEE Comput Soc Bioinform Conf* 2: 326-336, 2003.
- Chen X: Curve-based clustering of time course gene expression data using self-organizing maps. *J Bioinform Comput Biol* 7: 645-661, 2009.

17. Kanehisa M and Goto S: KEGG: Kyoto encyclopedia of genes and genomes. *Nucleic Acids Res* 28: 27-30, 2000.
18. Huang DW, Sherman BT, Tan Q, Collins JR, Alvord WG, Roayaei J, Stephens R, Baseler MW, Lane HC and Lempicki RA: The DAVID Gene Functional Classification Tool: A novel biological module-centric algorithm to functionally analyze large gene lists. *Genome Biol* 8: R183, 2007.
19. Eickhoff SB, Schleicher A, Scheperjans F, Palomero-Gallagher N and Zilles K: Analysis of neurotransmitter receptor distribution patterns in the cerebral cortex. *Neuroimage* 34: 1317-1330, 2007.
20. Verdoni AM, Schuster KJ, Cole BS, Ikeda A, Kao WW and Ikeda S: Deletion of serum response factor rescues the cornea defects caused by the loss of actin depolymerizing factor (ADF/Destrin) in mouse. *Genetics*: July 6, 2010 (Epub ahead of print). doi: 0.1534/genetics.110.117309.
21. Bai S, Nasser MW, Wang B, Hsu SH, Datta J, Kutay H, Yadav A, Nuovo G, Kumar P and Ghoshal K: MicroRNA-122 inhibits tumorigenic properties of hepatocellular carcinoma cells and sensitizes these cells to sorafenib. *J Biol Chem* 284: 32015-32027, 2009.
22. Choi H, Kim KR, Lee JH, Park HS, Jang KY, Chung MJ, Hwang SE, Yu HC and Moon WS: Serum response factor enhances liver metastasis of colorectal carcinoma via alteration of the E-cadherin/b-catenin complex. *Oncol Rep* 21: 57-63, 2009.
23. Dos Remedios C, Chhabra D, Kekic M, Dedova I, Tsubakihara M, Berry D and Nosworthy N: Actin binding proteins: Regulation of cytoskeletal microfilaments. *Physiol Rev* 83: 433-473, 2003.
24. Ikeda S, Cunningham LA, Boggess D, Hawes N, Hobson CD, Sundberg JP, Naggert JK, Smith RS and Nishina PM: Aberrant actin cytoskeleton leads to accelerated proliferation of corneal epithelial cells in mice deficient for destrin (actin depolymerizing factor). *Hum Mol Genet* 12: 1029-1036, 2003.
25. Miano JM, Long X and Fujiwara K: Serum response factor: Master regulator of the actin cytoskeleton and contractile apparatus. *Am J Physiol Cell Physiol* 292: C70-C81, 2007.
26. Kanellos G, Zhou J, Patel H, Ridgway RA, Huels D, Gurniak CB, Sandilands E, Carragher NO, Sansom OJ, Witke W, *et al*: ADF and Cofilin1 control actin stress fibers, nuclear integrity, and cell survival. *Cell Rep* 13: 1949-1964, 2015.
27. Maciver SK and Hussey PJ: The ADF/cofilin family: Actin-remodeling proteins. *Genome Biol* 3: reviews3007, 2002.
28. Carlier MF, Laurent V, Santolini J, Melki R, Didry D, Xia GX, Hong Y, Chua NH and Pantaloni D: Actin depolymerizing factor (ADF/cofilin) enhances the rate of filament turnover: Implication in actin-based motility. *J Cell Biol* 136: 1307-1322, 1997.
29. Ichetovkin I, Grant W and Condeelis J: Cofilin produces newly polymerized actin filaments that are preferred for dendritic nucleation by the Arp2/3 complex. *Curr Biol* 12: 79-84, 2002.
30. Khachigian LM and Collins T: Inducible expression of Egr-1-dependent genes a paradigm of transcriptional activation in vascular endothelium. *Circ Res* 81: 457-461, 1997.
31. Gineitis D and Treisman R: Differential usage of signal transduction pathways defines two types of serum response factor target gene. *J Biol Chem* 276: 24531-24539, 2001.
32. Zhang W and Liu HT: MAPK signal pathways in the regulation of cell proliferation in mammalian cells. *Cell Res* 12: 9-18, 2002.
33. Sumimoto H, Imabayashi F, Iwata T and Kawakami Y: The BRAF-MAPK signaling pathway is essential for cancer-immune evasion in human melanoma cells. *J Exp Med* 203: 1651-1656, 2006.
34. Breuss JM, Gallo J, DeLisser HM, Klimanskaya IV, Folkesson HG, Pittet JF, Nishimura SL, Aldape K, Landers DV, Carpenter W, *et al*: Expression of the beta 6 integrin subunit in development, neoplasia and tissue repair suggests a role in epithelial remodeling. *J Cell Sci* 108: 2241-2251, 1995.
35. Alam N, Goel HL, Zarif MJ, Butterfield JE, Perkins HM, Sansoucy BG, Sawyer TK and Languino LR: The integrin-growth factor receptor duet. *J Cell Physiol* 213: 649-653, 2007.
36. Garlick DS, Li J, Sansoucy B, Wang T, Griffith L, FitzGerald T, Butterfield J, Charbonneau B, Violette SM, Weinreb PH, *et al*: $\alpha(V)\beta(6)$ integrin expression is induced in the POET and Pten(*pc*^{-/-}) mouse models of prostatic inflammation and prostatic adenocarcinoma. *Am J Transl Res* 4: 165-174, 2012.